DYNAMICS OF CARBON DIOXIDE BUBBLE SHRINKAGE IN MICROCHANNEL FLOW DETERMINES MASS TRANSFER IN PHYSICAL SOLVENTS

Milad Abolhasani[*], Eugenia Kumacheva[**] & Axel Günther[* a)]
[*]*Department of Mechanical and Industrial Engineering, University of Toronto, Toronto, M5S 3G8, Canada*
[**] *Department of Chemistry, University of Toronto, Toronto, M5S 3H6, Canada*

Summary We investigate the confined flow of long carbon dioxide (CO_2) bubbles in physical solvents. By determining the shrinkage of the bubble length we measure CO_2 mass transfer at Capillary numbers ranging from 5×10^{-4} to 6×10^{-3}. Our experimental strategy utilizes an image-based feedback approach that allows us to systematically vary flow parameters that otherwise adjust dynamically (i.e., the length of bubbles, the distance between them, as well as the bubble velocity). we show that the dimensionless CO_2-dimethyl carbonate (DMC) mass transfer coefficient increases by increasing the capillary number with a slope of 0.71 in a log-log plot.

INTRODUCTION

The transport of carbon dioxide (CO_2) across gas-liquid interfaces and, upon dissolution, in a liquid is of profound relevance for flow problems ranging from the microscale (e.g., CO_2 bubbles in microreactors [1] , as contrast agents for biomedical imaging and in carbonated beverages, e.g., Tsingtao Beer) to geophysical scales (e.g., carbon transport at ocean surface [2] and within the oceans). We study the dissolution of long CO_2 bubbles that immersed in a physical solvent (i.e. there is no chemical reaction between the dissolving gas and the liquid), and confined by a long, gas-impermeable microchannel [3,4]. No gas is dissolved at the initial location where bubbles are formed through passive breakup at a T junction. With increasing distance from the T-junction, the bubble length reduces until an equilibrium length is reached. The latter is controlled by the solubility of the gas in the considered solvent at a given temperature. Our contribution focuses on the dynamic effect of gas dissolution in the liquid. Using an automated microfluidic platform, we experimentally measure the size evolution of bubbles for a wide range of flow conditions to determine the dimensionless mass transfer coefficient, the Sherwood number, *Sh*, as a function of the capillary number, *Ca*. Experimental results of Bercic and Pintar [5] showed that the segmented flow parameters affecting *Sh* are liquid slug length, L_S, and the bubble velocity, U_B. On the other hand, in a microscale segmented flow format, the non-linear nature of multiphase flows relates externally selected parameters such as liquid flow rate, Q_L, and the gas inlet pressure, P_G, to a dynamically selected set of dependent parameters, the gas bubble length, L_B, L_S, and U_B. In this study, we will use an automated image-based technique (Matlab) to study the role of initial U_B on *Sh* while maintaining the other initial segmented flow parameters the same (using an initial parameter screening).

EXPERIMENTAL

Figure1a schematically shows the size evolution of initially uniformly sized gas bubbles that are separated by uniformly sized liquid bridges (slugs) of a physical solvent. We consider 'long bubbles', i.e., the bubble length is greater than the width of the confining microchannel, and can identify two phenomena affecting the bubble length. Bubbles shrink due to the dissolution of the gas in the liquid (red color) and expand in what can be assumed an isothermal process due to the pressure drop in the microchannel (blue color).

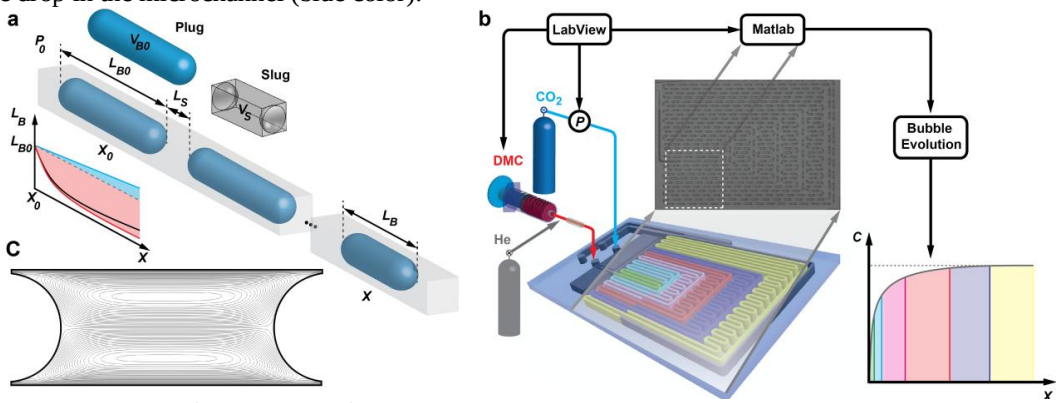

Fig1. (a) Schematic illustration of the evolution of the CO_2 bubble length bubble along the microchannel, and the corresponding volumes to a gas bubble and liquid slug that were used in the calculations are shown. Superposition of the measured bubble size evolution, black line, the bubble expansion due to the pressure drop, highlighted with blue, and the bubble shrinkage only due to the dissolution, highlighted with red, is illustrated. (b) The experimental setup and the flowchart to measure the dissolved gas concentration using the segmented flow images are shown. (c) Illustration of the velocity field inside the liquid as indicated by the streamline pattern obtained from a 2D numerical simulation. (simulation boundary conditions: moving walls at the top and bottom with a velocity of 20 mm/s, free slip boundary condition for the bubble caps, and periodic boundary conditions for the 4 liquid film sections at the corners).

[a)] Corresponding author. Email: axel.guenther@utoronto.ca.

After accounting for the isothermal expansion, the image-based measurement of the volume reduction of the dissolved gas determines its bulk concentration in the liquid. The bubble velocity (dynamically varying) and equilibrium gas concentrations (i.e. concentration of the saturated liquid slug) can be employed to calculate *Sh* and mass transfer time, using the relationship, $Sh=((d_h U_B/(x \cdot D)\ ln[(C^*(P,T)-C(P,T))/(C^*(P,T)-C_0)]$, where $C^*(T,P)$ is the saturated gas concentration in the liquid slug, C_0 is the initial gas concentration in the liquid, d_h is the channel hydraulic diameter and *D* is the gas diffusivity in the considered solvent. As shown in Fig. 1c, the liquid elements in contact with the gas bubble caps will be replaced by the fresh liquid from the liquid bulk. The dissolution in the direction normal to the gas-liquid interface, and also through the liquid streamlines into the middle of the recirculation are only diffusion controlled
Figure 1b shows the automated microfluidic platform consisting of an automated syringe pump and a digital pressure regulator (controlled via LabView) in combination with a helium jacket to maintain the initial CO_2 concentration inside dimethylcarbonate (DMC) zero. Silicon-based microfluidic devices were fabricated using standard microfabrication processes [1]. Six different downstream channel sections were routed through a single field of view as illustrated with different colors in Fig. 1b. The field of view used for measuring bubble shrinkage is indicated with dashed-lines in white color inside an image of the segmented flow across the entire microfluidic chip.

RESULTS

Figures 2a and b show how the bubble length, slug length and bubble velocity (all evaluated in close proximity of the location of bubble breakup after a T-junction) are interrelated. The slug length evolution along the same line on the initial working space used to maintain the initial bubble length constant is shown in Fig. 2c. After $U_B=110$ *mm/s*, L_S becomes constant, therefore the measured *Sh* values after this point would be only affected by the bubble velocity. Figure 2d shows the dimensionless gas-liquid mass transfer coefficient of CO_2-DMC pair as a function of the dimensionless bubble velocity for fixed initial values of L_B and L_S. Our unique experimental setup allowed the bubble velocity (and therefore Ca) to be varied over more than one order of magnitude. The corresponding mass transfer times were ranging from 33 to 250 ms. A slope of 0.71 was obtained for the dimensionless mass transfer coefficient as a function of *Ca* number, indicating the mass transfer rate was increased by increasing the bubble velocity.

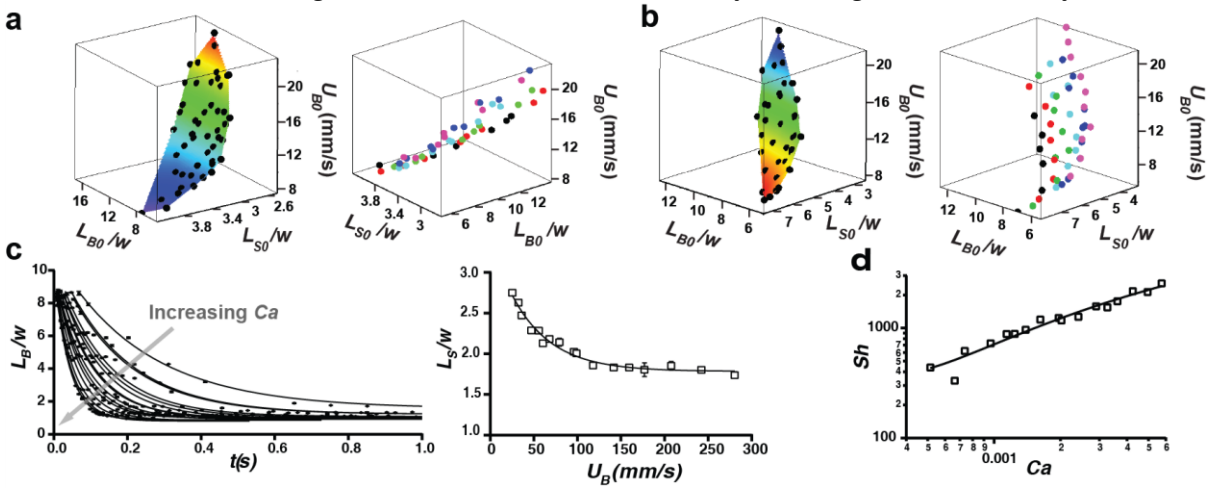

Fig2. (a) Interrelationship of initial bubble length (L_{B0}), initial liquid slug length (L_{S0}) and initial bubble velocity (U_{B0}) for flow of uniformly sized CO_2 in the physical solvent dimethylcarbonate (DMC) where the surface indicates a best fit to the measurement data. (b) Data obtained for the case of a weakly soluble gas-liquid pair: dissolution of He bubbles in DMC. (c) CO_2 bubble length evolutions for the same initial bubble length and different bubble velocities. DMC slug length evolution while increasing CO_2 bubble velocity for the same initial bubble sizes. (d) The measured Sherwood numbers for CO_2-DMC mass transfer as a function of Ca for constant initial CO_2 bubble sizes of $L_{B0}/w=8.5$ with a slope of 0.71.

CONCLUSIONS

We demonstrated an image-based strategy for determining mass transfer behaviour by tracking the size evolution of CO_2 bubbles in physical solvents. The fully-automated nature of the demonstrated approach allows us to screen a wide range of different flow conditions and gas-liquid pairs and systematically assess how the dimensionless mass transfer scales with different flow conditions in the flow of long bubbles through a microchannel.

References

[1] Abolhasani, M. et al., Automated microfluidic platform for studies of carbon dioxide dissolution and solubility in physical solvents, *Lab Chip*, DOI: 10.1039/C2LC21043F, 2012.

[2] Banerjee, S., The air-water interface: Turbulence and scalar exchange. *Transport at the Air-Sea Interface*, **11**(87-101), 2007.

[3] Bretherton, F.P., The motion of long bubbles in tubes, *Journal of Fluid Mechanics*, **10**(166-188), 1961.

[4] Gunther, A. and K.F. Jensen, Multiphase microfluidics: from flow characteristics to chemical and materials synthesis. *Lab Chip*, **6**(1487-1503), 2006.

[5] Bercic, G. and A. Pintar, The role of gas bubbles and liquid slug lengths on mass transport in the Taylor flow through capillaries. *Chemical Engineering Science*, **52**: 3709-3719, 1997.